In Vitro Interactions between the Two Mitochondrial Membrane Proteins VDAC and Cytochrome *c* Oxidase[†,‡]

Inge Roman,[§] Jurgen Figys,[§,||] Griet Steurs,[§,||] and Martin Zizi*[,§,||]

Department of Physiology, FYSP-Neurophysiology, Vrije Universiteit Brussel (VUB), Brussels 1090, Belgium, and Division Studies, Epidemiology and Biostatistics, Department of Defense, Brussels 1120, Belgium

Received April 13, 2005; Revised Manuscript Received July 16, 2005

ABSTRACT: VDAC, a mitochondrial outer membrane channel, is involved in the control of aerobic metabolism and in apoptotic processes via numerous protein−protein interactions. To unveil those interactions, we screened a human liver cDNA library with the phage display methodology optimized to target VDAC reconstituted into a membrane environment. One positively selected clone yielded a sequence matching a part of the subunit I of human cytochrome *c* oxidase (COX), a mitochondrial inner membrane enzyme. Such putative interaction was never reported before. This interaction proved to be functional as evidenced by the effect of the human and yeast isoforms of VDAC on the oxidation of cytochrome *c* by the pure holoenzyme and by the effect of the COX epitope on VDAC permeability. Our results providing four independently obtained evidences of VDAC−COX interaction in vitro, would support a novel and potentially important level of mitochondrial regulation given the respective locations and functions of both proteins.

VDAC[1] is a multifunctional protein located in the mitochondrial outer membrane where it can serve either as a channel, a receptor, or a regulatory molecule. It is convincingly involved in the control of aerobic metabolism, as it forms the main protein pathway for metabolite diffusion across the mitochondrial outer membrane (*1*), and serves also as an anchoring and/or activating point for enzymes such as hexokinase, glucokinase, and glycerol kinase (reviewed in ref *2*). It can thus regulate both the outer membrane permeability to the anionic metabolites and the activity of some of the key metabolic enzymes generating those metabolites in the cytosol. Although the precise structure of the VDAC protein is still a matter of debate, all the data are consistent with a monomeric protein channel with most of its protein mass embedded within the membrane leaving only a few short loops to interact with other proteins (*3*). Via numerous protein−protein interactions with members of the Bcl-2 family, the VDAC channel can integrate various cellular signals during the apoptotic processes (*4*, *5*). Together with the adenine nucleotide translocator (ANT), some—but not all—of the mitochondrial VDAC proteins presumably form one type of contact sites between the two mitochondrial membranes; such sites would form the permeability transition pore (PTP) by binding cyclophilin D (*6*−*8*). Such complex interactions highlight the various yet-to-be-understood links between apoptosis and metabolism. Further, VDAC is also known to interact with cytoskeletal elements such as MAP2 (*9*), gelsolin (*10*), and G-actin (*11*) and may thus partake in mitochondrial or cellular motility. It interacts with other enzymes such as the Kringle 5 domain of human plasminogen (*12*), endothelial nitric oxide synthase (*13*), and with itself (*14*, *15*). These multiple and complex protein−protein interactions—most of them indirectly obtained—warrant a systematic search of the VDAC interacting map of proteins or *interactome*. Indeed, much of the information pertaining to the many reported VDAC−protein interactions relies on indirect evidences or on knockout experiments that do not always yield unequivocal interpretations. Depending also on the experimental (i.e., reductionist) conditions, some interactions may be favored over others or may even be due to altered protein folds, depending on the test conditions.

To find the various proteins binding to VDAC (as close as possible to its native fold), we reconstructed the VDAC protein into liposomes, using well-accepted reconstitution protocols yielding functional channels in lipid bilayers. These liposomes were then fixed on a Biacore sensor chip, and a liver cDNA library was screened with the Phage Display technique within the biosensing device itself. One of the first cDNA sequences (among many) selected by this setup was a part coding for subunit 1 of cytochrome *c* oxidase (COX), the fourth complex in the respiratory chain. To assess the possible physiological relevance of such interaction, its functional effects were assayed. Hence, we report that

[†] This work was supported by Grants WB01 and WB03 from Belgium Department of Defense. J.F., G.S., and M.Z. (partim) are supported by the Belgian DoD.

[‡] Patent protection has been requested for some of the work reported here.

* To whom correspondence should be addressed: E-mail, martin.zizi@vub.ac.be; telephone, +32 (0)2 477 4434; fax, +32 (0)2 477 4568.

[§] Vrije universiteit Brussel (VUB).

[||] Department of Defense.

[1] Abbreviations: VDAC, voltage-dependent anion channel; HVDAC, human voltage-dependent anion channel; YVDAC, yeast voltage-dependent anion channel; COX, cytochrome *c* oxidase; Cyt *c*, cytochrome *c*; ANT, adenine nucleotide translocator; PTP, permeability transition pore.

10.1021/bi050674s CCC: $30.25
Published on Web 09/07/2005

nanomolar concentrations of VDAC markedly increase the COX-dependent oxidation of cytochrome *c* (Cyt *c*), its natural substrate. The enzymatic data are consistent with an uncompetitive process. Both yeast VDAC1 and its ortholog, human VDAC1, but not the human VDAC2 were effective. Alternatively, in a VDAC−proteoliposomes permeability assay, COX decreases the VDAC permeability to poly(ethylene glycol) (PEG 800). Such reciprocal functional influences between the two proteins would indicate a possible in vivo interaction.

EXPERIMENTAL PROCEDURES

Reagents. All reagents were analytical grade. Crystal grade Cytochrome *c* oxidase was kindly provided by Dr. Verkhovsky, Helsinki, Finland. VDAC from yeast or yeast-expressed human VDAC 1 and 2 isoforms were purified to near homogeneity according to the method of De Pinto et al. (*16*, *17*). Phospholipids were L-a-phosphatidyl choline Type II-S from soybean, asolectin (Sigma-Aldrich, Belgium). Running buffer HBS-N (0.15 M NaCl and 10 mM HEPES, pH 7.4) was filtered and degassed (Biacore).

Liposome Preparation. Phospholipids (asolectin, 1.52 mg) with 20% cholesterol (0.3 mg) were dissolved in 1 mL hexane in a 10 mL round-bottom flask. These lipid conditions are known to yield functional VDAC channels upon reconstruction (*18*−*21*). A thin lipid film was deposited by evaporation of hexane under a filtered N_2-stream (0.22 μm filter). One milliliter of experimental buffer (1 M KCl, 5 mM $CaCl_2$, and 10 mM HEPES, pH 7.2, filtered through 0.22 μm filters) was added to obtain a 20 mM suspension, and multilamellar vesicles (MLV) were formed by extensive vortexing. The high KCl concentration is needed for the ensuing VDAC reconstitution. The lipid suspension was then submitted to 4 freeze−thaw cycles and to a 10 s sonication period to yield large unilamellar vesicles (LUV). Finally, the size of these vesicles was homogenized by pushing the suspension 25−30 times through a 100-nm polycarbonate filter in a mini extruder (Avanti Polar Lipids, Inc.).

VDAC Proteoliposomes. Using lipids and protocols that routinely and successfully reconstruct VDAC into planar lipid membranes, we reconstructed VDAC into liposomes. Those VDAC−liposomes were obtained by diluting (1:3, v/v) of the previous liposome (LUV) suspension with 50% experimental buffer (as above) and by adding twice (separately) 50 μL of a purified VDAC-containing solution (1 mg/mL VDAC in 5 mM Tris pH 7, 0.5 mM EDTA, 2.5 mM KH_2PO_4, and 25 mM KCl/1% Triton) to 400 μL of liposomes, waiting each time 10 min for VDAC to insert. The VDAC proteoliposomes were then diluted (1:3, v/v) in an appropriate buffer (30 mM KCl and 10 mM HEPES, pH 7.4, filtered through 0.22 μm filters) to obtain a final VDAC−LUV suspension with a low final Triton concentration (0.05%), a physiological osmolarity (300 mOsm), and a lipid concentration of 1 mM. Blank liposomes (without any protein) were made and diluted in the same fashion.

Liposome Immobilization on a L1 Sensor Chip. Vesicles were captured on the L1 sensor chip as previous described (*22*). Shortly, the surface of a L1 sensor chip was cleaned by a 2-min injection of 20 mM Chaps at a flow rate of 20 μL/min, followed by the "extra-clean" rinsing routine. HBS-N was used as running buffer after filtration and degassing. Liposomes (80 μL, 1 mM of lipids) were then immediately injected at a flow rate of 2 μL/min. The fixed lipid layer was then washed at a flow rate of 100 μL/min with sodium hydroxide (10 mM, 50 μL). In the case of VDAC−liposomes, 120 μL of a proteoliposome solution (1 mM P-lipids) at the same flow rate was used. Following a 2−12 h long control period (running buffer at 5 μL/min) to ascertain the stability of the fixed phase in the biosensor chamber, the degree of coverage of the chip's surface was determined by the ratios of the background reading signals (in relative resonance units, RU) in the presence or the absence of liposomes. The uncovered chip surface was then blocked with bovine serum albumin (BSA) (0.1 mg/mL, injection of 25 μL at 5 μL/min) (*23*).

Biopanning of the Phage Library against VDAC−Liposomes. The pre-made T7-Select Liver library (Novagen, Madison, WI) was used for selecting the phages displaying expressed epitopes binding to VDAC. This cDNA library expresses its inserts fused to the C-terminus of the T7 gene 10B major capsid protein, with an average of 10 copies displayed per virion, and inserts range from 300 to 3000 bp. The biopanning rounds were performed in a Biacore 2000 instrument (Biacore AB, Uppsala, Sweden) using a L1 sensor chip and HBS-N (above) as running buffer.

Phage Selection. To select for phages that bind to VDAC, the initial library was amplified and injected at a very low flow rate (1 μL/min) over a chip covered with VDAC−liposomes (∼5000 RU level). Such low flow rate allows a better competition between the viral particles for the binding sites. To filter out the phages bearing plain lipophilic epitopes or epitopes targeted to BSA, i.e., to increase the specific signal-to-noise ratio, the phage solution is first flushed at the same flow rate over three flow cells covered with blank liposomes (covered at ∼7000 RU level) and blocked with BSA before being allowed to reach the fourth flow cell covered with VDAC−liposomes. A titer of 10^9 phages/100 μL was used to cover the whole range of the library sequence space (10^7variants/mL according to the manufacturer's manual). Such panning rounds were repeated three times.

Phage Elution. Following the competition and presumably the binding phase, the reaction chamber was briefly washed with buffer (5 min at 1 μL/min) to remove any unbound or poorly bound material. To recover VDAC-binding phages based on different dissociation rates, collections over sequential time intervals were performed from flow cell no. 4. A fixed amount of buffer was injected at 1 μL/min and recovered in full every 40 min; this was performed four times yielding thus four fractions separating the phages based on their dissociation rate constants. As a control, the same procedure was used over flow cell no. 3 (liposome-binding phages). As prior to the next panning round the chip surface had to be regenerated, it was cleaned twice with 20 mM Chaps to remove any liposomes and/or proteoliposomes, and another immobilization procedure was performed.

Phage Amplification and Titration. Phage titers were determined by infection of 250 μL of BLT5615 cells and harvested in the presence of carbenicillin (50 μg/mL), with 100 μL of a 10-fold dilution of the eluted phages. The cell−phage samples were added to 3 mL H-top agar containing 4 mM IPTG and plated on LB agar supplemented with carbenicillin. IPTG is required to induce the production of the 10A capsid protein of the T7 phages. The plates were

left overnight at room temperature; the number of plaque forming units (PFU) was counted for all samples.

To amplify the phages between each selection round, 10 mL of BLT5615 cells (harvested at log phase in the presence of carbenicillin and IPTG 1mM) was infected with 20 μL of phage eluate. Incubation for 1.5 h at 37 °C in a sterile chamber caused complete lysis of the cells. Cell debris was removed by centrifugation for 10 min at 8000*g*, and 15% chloroform was added to the phage-containing supernatant to clear the sample from unprecipitated debris. This step was found essential to decrease microfluidic (chip) and macrofluidic (catheters) problems within the biacore machine. The catheters of the machine were changed between rounds of testing. The phage samples were further purified by PEG precipitation (phages/PEG 6000, 50% soln, 1:6 v/v) and finally dissolved in HBS-N. Phage titers following amplification were determined as described above.

Affinity Tests of the Selected Phage Populations. To evaluate the binding of phage populations selected from a surface-displayed library, affinity tests were performed within the SPR device (*24*). The L1 sensor chip was covered either with VDAC−liposomes or liposomes and blocked (see above). Coverage of the chip surface was kept high, typically around 7000 RU for VDAC−liposomes and 8000 RU for liposomes. Amplified phage populations at a concentration of 3.3×10^{10} PFU/mL were injected separately over the two surfaces at a high flow rate (30 μL/min) for 2 min, after which dissociation curves were followed for 10 min. Prior to each injection of phages, a buffer-only control run was performed.

Single Clone Amplification. A portion of the top agarose of individual plaques was scraped and used to infect 10 mL of BLT5615 cells as described above.

PCR Amplification of cDNA Inserts and Sequencing. A total of 5 μL of the amplified individual phages was dispersed in 100 μL of EDTA (10 mM, pH 8). The samples were vortexed, heated for 10 min at 65 °C, and cooled to room temperature. After a 10 min centrifugation period (14 000*g*) the phage lysates were added to the PCR mix (Taq PCR Mastermix, Qiagen) containing the T7Forward and the T7Reverse oligonucleotide primers. The PCR conditions after a hot start (10 min at 80 °C) were 94 °C for 50 s, 50 °C for 1 min, and 72 °C for 1 min (35 cycles), followed by 6 min at 72 °C. Finally the samples were purified (Qiaquick purification kit) and controlled by electrophoresis on a 1% agarose gel. The PCR amplified DNA was submitted for DNA sequencing with the T7Forward primer.

Cytochrome c Oxidase Assay. Functional effects of VDAC on COX were assayed by following the oxidation of reduced Cyt *c* at 550 nm by COX. Cyt *c* was brought to its fully reduced state with sodium dithionite (22:1, w/w) in a buffer without detergent (Tris-HCl 10 mM, pH 7.0, and KCl 120 mM). YVDAC was dissolved in 50 mM KCl, 1 mM EDTA, 10 mM HEPES, and 1% Triton X-100 by gel filtration, and further dilutions were made in the same buffer. HVDAC1 and HVDAC2 were dissolved in 25 mM KCl, 0.5 mM EDTA, 5 mM Tris, 1% Triton X-100, and 6% DMSO. Fixed volumes of the VDAC dilutions were added to fixed volumes of COX (in 20 mM HEPES, 0.1% dodecyl maltoside), to avoid any detergent concentration differences at the various VDAC doses, and stabilized on ice for 10 min. This mix was added to fully reduced Cyt *c* with final reagents concentrations of 0.2 μM COX, 109 μM Cyt *c*, and VDAC ranging from 30 nM to 1 μM. The final buffer composition was 9.6 mM Tris-HCl, 0.635 mM HEPES, 116 mM KCl, 0.023 mM EDTA, and a constant detergent concentration of 0.025% (0.002% DM, 0.023% Triton X-100).

VDAC Permeability Assay. VDAC−liposomes (LUV) were prepared as described above, except for an additional dilution step (1:2, v/v) in 0.75 M KCl, and stabilized on ice for 30 min. Fixed volumes of phages (2×10^9−2×10^{10} phage particles, controlled by titration) where added to 200 μL of a proteoliposomes solution, the mix was stabilized for 10 min, and 10 μL of a 200 mM stock of PEG 800 (final concentrated 10 mM) was added right before reading. Volume changes were recorded as variations in light scattering with a Biorad microplate reader at 400 nm.

RESULTS

Positive Clone Selection. To select for physiologically expressed epitopes that bind to VDAC in the nearest to its native conformation we had to modify the phage display methodology. The channel protein was functionally reconstructed in liposomes; protocols and conditions were used that allow to study the channel function (*18*−*21*). Those proteoliposomes were then anchored on the surface of a SPR chip. The biopanning rounds were performed inside the chamber of a Biacore 2000 device using the procedure described in the experimental procedures. Starting with a phage-expressed cDNA library (titer 10^7 variants) iterative rounds of selection were performed, using phages obtained by the controlled elution of near permanent binders as input (elution fraction no. 4 in Figure 1A). This fraction would correspond to phages that are released from their binding site with a time course well above 3 h. It is important to note that all VDAC-selective binding occurred only in the fourth flow cell of the device (containing VDAC reconstructed into liposomes) and that aspecific phospholipid binding was minimized by running the samples first through three flow cells (covered with plain liposomes) (Figure 1A). Between rounds, the positively selected phages were amplified to reach an input titer value of 10^9 viral particles for the next round. We controlled the resulting bulk affinity of our selected phage populations in separate sets of experiments. In Figure 1B, we show a measure of such affinities as the binding curves of a positive eluate during 2 subsequent rounds of panning. Comparison of both panels demonstrates that selectivity for VDAC versus phospholipids increases with the rounds. From such a phage pool after 3 such rounds, single clones were obtained by diluted titration, picked up, and amplified for sequencing and identification.

Clone Identification. The DNA insert of one of the positive clones yielded a 224 bp sequence. This sequence perfectly matched a portion of the *Homo sapiens* mitochondrial genome (bp 6209−6423) coding the cytochrome *c* oxidase subunit I (*25*) and corresponding to the region between amino acids 103−172 (Figure 2). From the crystal structure of the chain A of the bovine heart cytochrome *c* oxidase (region is 93% identical in human and bovine isoforms), it can be derived that our binding domain spans a β-turn region and its two adjoining α-helices (helices 7 and 8) (*26*).

Binding of Pure COX to Pure VDAC. To evidence a direct interaction between COX and the channel protein, the binding

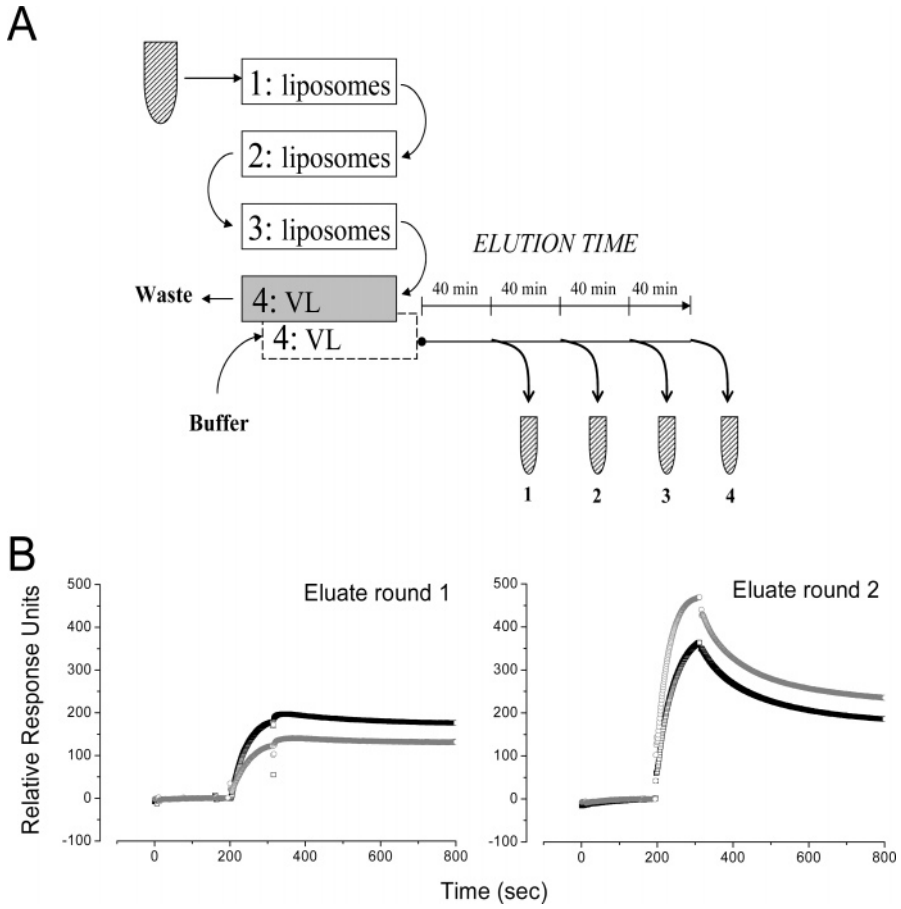

FIGURE 1: SPR-based experimental panning strategy and its quality control. (A) Our experimental scheme. The input phages (10^9 phages/100 μL) were fed into the SPR device at a very slow flow rate (1 μL/min) to ensure an optimal competition between the phages particles. Aspecific Darwinian selection was minimized by first forcing the phages on the three first flow cells of the SPR chamber covered with plain liposomes only, then feeding them in the fourth flow cell covered with VDAC proteoliposomes. After rinsing with HBS-N, bound phages were eluted as four different fractions. (B) The compared affinities of one such eluate following the first (left panel) or the second (right panel) selection round as measured by SPR in separate experiments. The curves represent the sensorgram data obtained by testing the positive phage eluate against plain liposomes (black open square) or against VDAC proteoliposomes (gray open squares). The VDAC-selective signal increases between the two rounds shown here as examples. The phages from the eluate collected after the first round were re-amplified before being injected in for the second round.

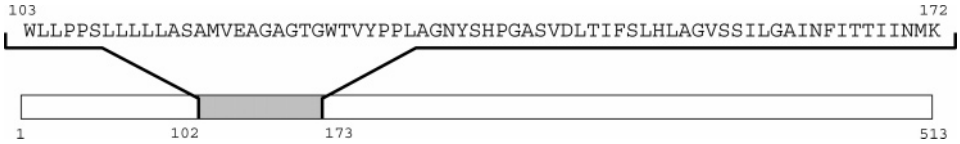

FIGURE 2: COX I region expressed by the VDAC-interacting clone. The VDAC-binding human COX I epitope is shown (shaded). The epitope spans residues 103−172. The residues 118−140 are reported facing the mitochondrial intermembrane space (from Swiss-Prot no. P00396); the rest of the sequence corresponds to transmembrane segments.

of the bovine holoenzyme (crystal grade) was measured against pure yeast VDAC reconstructed into proteoliposomes and fixed on the surface of a sensor chip.

In Figure 3, three sensorgrams of such direct interactions are shown. For each dose of the holoenzyme, the binding for VDAC−liposomes was preferred against pure liposomes.

Functional Effects of VDAC on COX. The binding between these two mitochondrial proteins was never reported before, but hinted at a probable functional interaction. Purified yeast VDAC enhanced the oxidation rate of Cyt *c* by the enzyme in a dose-dependent manner. Initial enzymatic velocities were multiplied by a factor of 3.5 by nano- to micromolar YVDAC (from 400 to 1400 mOD/min) (Figure 4A). Identical curves were obtained whenever VDAC was preincubated with COX or with Cyt *c*. As to perform such experiments, some low levels of detergent have to be present, and as cytochrome oxidase function is sensitive to detergent (*27*, *28*; control data, not shown), we were extremely careful to keep the detergent concentration constant at all the VDAC concentrations tested. The spontaneous oxidation of Cyt *c* in our assay conditions was also controlled and found to be 1% per hour.

The selective nature of this interaction was further evidenced by performing identical experiments using the two main human VDAC isoforms (HVDAC1 and HVDAC2). In Figure 4B, we show that both YVDAC1 and HVDAC1, at identical protein concentrations, are effectively enhancing the COX enzymatic activity, whereas HVDAC2 is not and remains close to the control curves. The enzyme activity remains unchanged in the presence of casein, a random

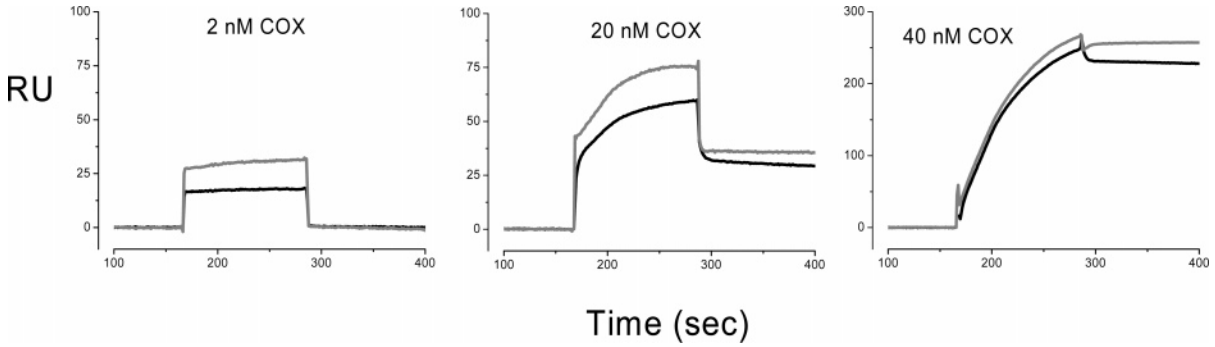

FIGURE 3: Direct COX−VDAC interactions. The affinity of three different concentrations of bovine COX on blank (black curves) or VDAC−liposomes (gray curves) as measured by SPR. Appropriate controls (matched SPR signals from respective COX-free solutions) were subtracted from the data; signal values were normalized as a function of the chip's surface covered by the proteoliposomes (SPR signal is proportional to the capture of the liposomes).

membrane-active protein, at higher concentrations (25 and 50 μg/mL, i.e., roughly around 1 and 2 μM, respectively) (data not shown).

From the data shown in Figure 4A, assuming a one-to-one interaction between the two proteins, a K_D value of 200 nM can be derived for VDAC (inset). When initial velocities are plotted as a function of various substrate concentrations for different VDAC levels (Figure 5, left panel) it can be shown that the enzymatic K_m values increased, with VDAC concentrations starting at 33.5 μM without VDAC added, up to 59 μM at the maximal VDAC dose tested. However, the ratio between the maximal velocity (V_{max}), obtained by hyperbolic fit of the data, and the K_m values remained nearly constant (see Table 1). This is further evidenced by the parallel plots on a Lineweaver−Burk chart (Figure 5, right panel). Such data are consistent with VDAC modifying the enzyme kinetics in an uncompetitive manner.

Effect of COX on VDAC. VDAC channel function can be assayed by measuring volume changes in proteoliposomes. Liposomes react to osmotic challenges by swelling or shrinking to a stable volume imposed by the new steady-state conditions. Figure 6 shows the responses of either liposomes or proteoliposomes following osmotic challenges. In panel A, an osmotic shock obtained by dilution of the buffer solution (initially KCl 2 M both inside and outside the liposomes, after shock 1 M outside) made the liposomes rapidly swell to a new stable value reflecting the set osmotic gradient (see lipos + shock). Without any osmotic shock, i.e., the addition of an identical volume of isotonic solution, the signal remains stable (see lipos − shock). With the protein successfully reincorporated into the liposomes, following the osmotic shock, after an initial signal disturbance, the liposomes do not swell noticeably (VDAC lipos + shock). This is due to the osmotic gradient equilibration that the VDAC pore would allow. Figure 6, panel B shows the proteoliposomes response following the addition of PEG to the cuvette. PEG 1500 is not permeable whereas PEG 800 is. The proteoliposomes response following the addition of 10 mM PEG 800 in the presence of either the naive phage library or the COX-bearing phage clone is markedly different (Figure 6, panel C). We see that the re-swelling slope is decreased; this is consistent with a decreased VDAC channel permeability for the osmoticant. The quality of the proteoliposomes is also evidenced by the shrinking and stable response obtained with a phage clone (no. 4L033) that fully blocks the VDAC channel, indicating that the measured permeability variations are not due to leaks in the proteoliposomes.

DISCUSSION

VDAC is known to interact with a whole set of proteins ranging from cytoskeletal elements, various enzymes, and apoptotic modulators to viral or bacterial proteins. As more and more of the VDAC *interactome* is being revealed, the central role and function of the mitochondrial channel start to stand out. To be able to determine the VDAC interactome as completely as possible, we adapted and modified a screening method based on the phage display methodology.

During this work, we used VDAC from yeast. Although it may seem an odd choice to perform screens on a *human* cDNA library, it offered us several advantages. Using wild-type baker's yeast, we could obtain both the massive quantities and the highly purified VDAC material that was needed to perform screening and testing of the phages. Further, the wild-type YVDAC1 can be more easily and reliably reconstituted within phospholipid membranes. The yeast and human VDAC1 protein sequences are roughly 50% homologous (28% identity and 17% similarity), but for interacting sites, it is more the three-dimensional positioning of key residues than the protein lineage, given by the primary structure, that is relevant. Although our approach is likely to miss some protein−protein interactions, it is even likely that highly critical interactions that are conserved through species might be selected by our study. In yeast, YVDAC1 is the housekeeping gene ortholog to human VDAC1; YVDAC2 is presumably not even a channel (*29*).

To bias our screening efforts toward physiologically expressed epitopes, we reconstructed the VDAC proteins into lipids using conditions and protocols that have been extensively used to functionally characterize the channel. As the orientation of the VDAC channel ought to be random following liposome incorporation (*15*), both cytosolic and mitochondrial epitopes are likely to be encountered during the screening process. In our strategy, flowing the batch of input phages over the control lipid surfaces prior to the VDAC liposomes minimizes the selection for aspecific binders. This strategy proved effective as evidenced by the affinity testing of the bulk output phage population.

From the positively selected phages originating from the high affinity binders after the third panning round, an individual clone was identified that carried a rather large

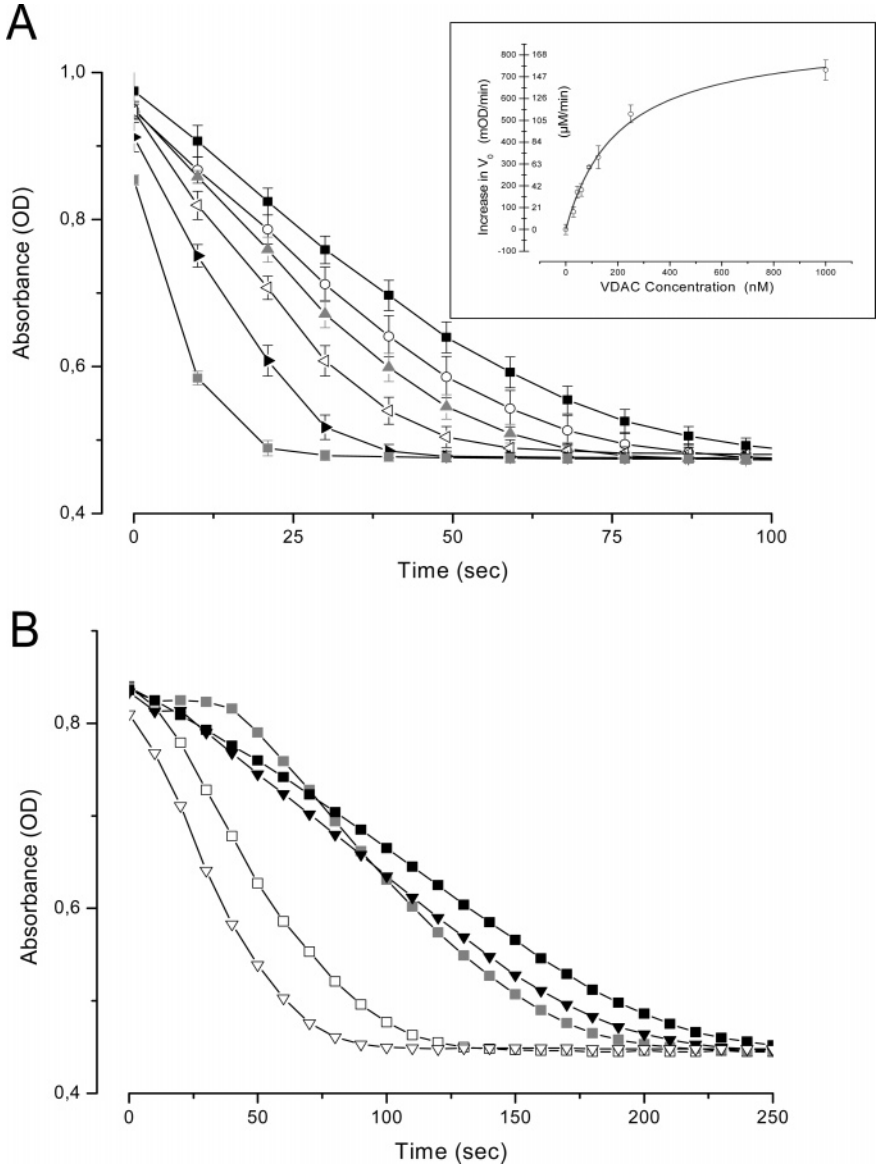

FIGURE 4: Pure VDAC enhances the oxidation of Cyt *c* by the COX holoenzyme. (A) Enzymatic oxidation of Cyt *c* (109 μM) by bovine COX (200 nM) increases up to 4-fold in the presence of increasing yeast VDAC concentrations (1 μM, gray squares; 250 nM, black triangles; 125 nM, white open triangles; 60 nM, gray triangles; 30 nM, open circles; and 0 nM, black squares). The oxidation was followed as a decrease in absorbance spectra at 550 nm in a Biorad plate reader. The plates were shaken during readings. Increases in initial velocities (V_0), derived from the initial linear fits of the absorbance data, are plotted as a function of VDAC concentration in the inset. Assuming a one-to-one interaction between VDAC and enzyme, the K_D, derived from the simple hyperbolic fit, is 200 nM (see inset). Assay buffer final composition was 9.6 mM Tris-HCl, pH 7, 0.635 mM HEPES, 116 mM KCl, 23 μM EDTA, and detergent concentration (0.002% dodecyl maltoside, 0.023% Triton X-100) was kept constant at all VDAC concentrations. Data are mean ± SE; each point represents the average of three independent experiments. (B) Identical experiments performed with either yeast VDAC (open triangles), human VDAC1 (open squares), and VDAC2 (grey squares). Identical doses (60 nM) of HVDAC1 and YVDAC1 enhance the enzymatic activity 3-fold, whereas HVDAC2 (60 nM) does not. The difference between YVDAC1 and HVDAC1 could be partly due to minor differences in the final salt concentrations between the two experiments (25 mM KCl for HVDACs vs 50 mM for YVDAC) resulting from protein purification. See the minor differences in the corresponding control curves (no VDAC, closed triangles for 50 mM KCl, closed squares for 25 mM KCl). Other conditions were identical to Figure 4A, except for the presence of 0.14% DMSO. This DMSO concentration was controlled in separate experiments with each VDAC isoform at identical concentrations and found to slightly decrease the VDAC effect on the COX activity (data not shown).

portion of the cytochrome *c* oxidase subunit I (COX subunit I, Swiss-Prot no. P00396) as a fusion protein on its envelope. Located within the mitochondrial inner membrane, COX is the terminal enzyme of the electron transport chain. The functions of this 205 kDa protein, i.e., Cyt *c* oxidation, electron transfer to oxygen, and proton pumping, are mainly ascribed to its subunits I and II, and three active redox metal centers are bound to its subunit I. The eukaryotic COX consists of a total of 13 subunits, three of which (subunit I, II, and III) are encoded in the mitochondrial DNA (*30*). These three subunits carry out the catalytic functions of COX and are highly conserved between Pro- and Eukarya (*31*). From our data, the interacting COX I region must be located between its residues 103−172. This region encompasses two transmembrane helical domains and a series of β-turns. More precisely, the region spanning residues 118−140 is reported facing the mitochondrial intermembrane space (*26*), while the other residues from our COX sequence are part of

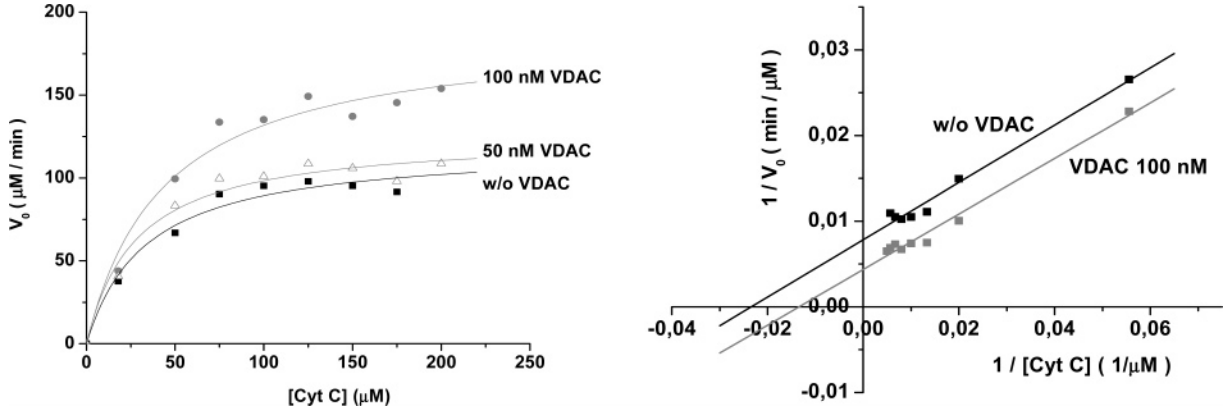

FIGURE 5: VDAC is an uncompetitive activator of COX. Initial velocities of the COX holoenzyme as a function of Cyt *c* concentrations for three different VDAC levels, none (black squares), 50 nM (open triangles), and 100 nM (closed circles). Assay conditions identical to Figure 4, except for the Cyt *c* concentration. In the left panel, the same data as a Lineweaver−Burk plot (at two different VDAC doses for clarity) evidencing that the interaction of Cyt *c* and VDAC for the COX enzyme is not competitive.

Table 1: COX Bovine Holoenzyme Kinetic Parameters Following VDAC Addition[a]

	V_{max} (μM/min)	K_M (μM)	V_{max}/K_M (1/min)
NO VDAC	125.2	33.5	3.7
VDAC 50 nM	132.5	28	4.7
VDAC 100 nM	198.7	44	4.5
VDAC 200 nM	224.3	59	3.8

[a] The values obtained by fitting the data from Figure 5 are listed here. It can be seen that the ratio between the enzyme maximal velocity (V_{max}) and the Michaelis−Menten constant (K_M) is relatively constant consistent with an uncompetitive process.

transmembrane regions (residues located up to 117 and at positions between 141 and 170). While partly buried, this whole region is not involved in the catalytic activity of the enzyme, nor is it reported being relevant for Cyt *c* binding. Although the main binding site for Cyt *c* lies in subunit II (*30*), several amino acids from the subunit I located at positions 50 and 221 seem involved in the molecular recognition (*32*) between the enzyme and the electron carrier. Concerning the interaction of the VDAC domain with COX, we can only propose that it has to be dependent on the few short extramembrane loops that the correctly folded VDAC protein allows (*33*, *34*). Direct binding between the two pure proteins was obtained and measured using surface plasmon resonance (Figure 3). Although the sensorgrams show that the COX holoenzyme binds more effectively to VDAC−liposomes than to plain liposomes, the specific signal remain poor. This is likely due to the fact that COX, an integral membrane protein, has, on its own, a very high affinity for phospholipids. From early biochemical studies on COX activity regained by a de-lipidified enzyme, one can deduce that around 150 nM of asolectin/mg oxidase can bind to the COX protein to yield the half-maximal measurable enzymatic activity (see Figure 2 in ref *35*). Regardless of the differences between our respective experimental conditions, this implies that asolectin and VDAC do actually compete for COX binding. As the molar fraction of chip-bound VDAC relative to the chip-bound phospholipid is likely very small, our experimental conditions within the biosensor were not well-suited for the determination of binding kinetics.

To further ascertain the eventual relevance of the VDAC−COX binding, i.e., to reveal a direct functional interaction between these two proteins, we performed an in vitro assay based on the enzymatic function of COX. While our assay conditions (116 mM KCl, 9.6 mM Tris-HCl, 0.635 mM HEPES, pH 7.2, 0.023 mM EDTA, and 0.025% detergent) were different from some of the authors, in terms of K^+ and dodecyl maltoside concentrations (*27*), our measured K_M of 33.5 μM compares very well with the already published values around 30 or 38 μM (*28*), or 16.7 μM (*27*). The situation is even more complex as some authors report two binding sites (high and low affinity), but in general, the published K_M values range between 20 and 60 μM (low affinity) and between 0.01 and 22 μM (high affinity) depending on the conditions (*36*−*38*). Thus, our COX assay using both bovine gene products (holoenzyme, Cyt *c*) and yeast or human VDAC(YVDAC, HVDAC) gave us enough signal-to-noise ratio to ascertain sizable variations in enzyme activity. A 3−4-fold acceleration in the rate of Cyt *c* oxidation could be measured using nanomolar concentrations of YVDAC. It must be pointed out that, in our assay, the detergent concentration was very carefully kept constant at all the VDAC doses tested (including in VDAC absence) to avoid the enzymatic results be due to detergent variations in the buffer. These variations are presumably due to differences in self-association of the various subunits in different detergent environments and conditions (*28*). Although from the literature we did not expect a problem with the presence of very low amount of Triton X-100 (*35*), this was a crucial variable to control as these amounts were close to its critical micellar concentration (CMC).

From our assay, performed in bulk phase conditions, we can derive an apparent K_D value of 200 nM of YVDAC for COX. The real value in the cell could be orders of magnitude lower as both these proteins have their free diffusion limited in the membrane bidimensional spaces and as the two mitochondrial membranes are very close to each other. Taken together, our enzymatic data are consistent with an uncompetitive activation process. Such processes where both V_{max} and K_M are increased are already described (*39*−*41*). The fact that HVDAC1, like the yeast isoform, can enhance the COX activity by a 3-fold factor, and that HVDAC2 does not, further argues in favor of a possible physiological relevance and highlights the diversity of the cellular functions performed by the various VDAC molecules. While the human VDAC1 is an ion channel and binds hexokinase, the human VDAC2 does not bind this enzyme (*42*). Further,

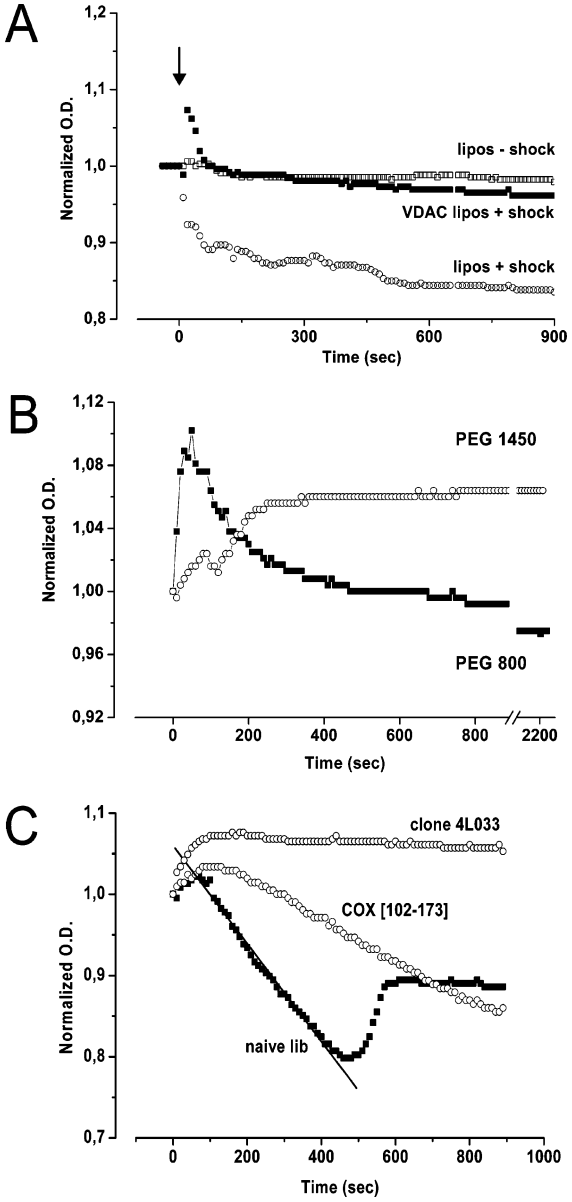

FIGURE 6: COX decreases VDAC permeability to PEG 800. (A) A series of control experiments is shown. VDAC proteoliposomes or blank liposomes are osmotically challenged by the dilution of the external buffer (KCl brought from 2 to 1 M by water addition). The volume changes of the liposomes (measured as light scattering at 400 nm) are plotted as a function of time. The VDAC pore allowing equilibration of any osmotic gradient for KCl, there are no marked differences due to the osmotic shock (closed squares) with the unchallenged liposomes (open squares). The plain liposomes behave osmometrically during the challenge (open circles). (B) Experiments following the addition of a fixed volume (10 μL) of 10 mM PEG 800 or 10 mM PEG 1500 used as osmoticant. Following an initial shrinkage due to the osmotic shock, the proteoliposomes re-swell only for the PEG 800, evidence that PEG 800 can re-equilibrate across the liposome membrane and is thus VDAC permeable (closed squares). This is not the case for the heavier colloid PEG 1500 in identical conditions (open circles). (C) An identical experiment performed using PEG 800 only. The swelling rate is different when the proteoliposomes, from the same batch, are preincubated and equilibrated with the initial naive phage library (closed squares), the pure COX-presenting phage clone (open circles), or a phage clone closing the VDAC channel (gray circles). The linear fit being proportional to the channel permeability, the difference in slope for the COX-presenting phage clone corresponds to a 2.3-fold decrease in VDAC permeability. This experiment was repeated with consistent results. For conditions, see Experimental Procedures.

HVDAC2 but not HVDAC1 has been reported to keep the pro-apoptotic BAK protein inactive (*43*), and Bax, another pro-apoptotic protein, seemingly regulates the BAK protein via HVDAC2 (*44*). COX rejoins thus other enzymes that can be activated upon binding to the VDAC1 isoform: hexokinase (*45*), mitochondrial creatine kinase (*46*, *47*), plasminogen (*12*), and eNOS (*13*), to cite a few.

Another functional evidence was obtained by measuring the effects of the COX epitope on the VDAC permeability after reconstitution into large unilamellar vesicles. Depending on the ionic and/or colloidal conditions, the volume of these proteoliposomes will vary and these variations in volume can be acquired as variations in light scattering measurable by a spectrophotometer (*48*). As the light scattering signal contains also information on the surface of the proteoliposomes, such experiments have to be perfectly calibrated; i.e., all variables are to be identical but the *nature* of the tested ligand. Taking advantage of the differential VDAC permeability displayed in our conditions by identical concentrations of PEG 800 and PEG 1500, we could reliably measure VDAC closure by the slope of the re-swelling of the proteoliposomes consecutive to the addition of a fixed concentration of a perfectly VDAC-permeable osmoticant. When the channel is closed or when PEG1500 is used, there is barely any re-swelling following the osmotic challenge. As our assay is sensitive to dilution effects, identical volumes of phage-containing solutions were always used for the experiments. The phage concentrations used in our experiments, as determined by titration, ranged between 1.5 and 0.15 nM. Such variations can be considered trivial regarding osmotic effects. We can clearly see that the phages bearing the COX sequence but not the naive phage particles decrease the slope of re-swelling. This would be consistent with the COX protein favoring VDAC closure.

Although our findings came about by in vitro experiments, the possible in vivo implications may be of great importance to cellular physiology. Given the respective locations, abundance, and roles of both interacting partners, this novel protein−protein interaction could hint at a novel type of contact site inside the mitochondrion. While we used one yeast VDAC protein as bait, we got binding of a large domain from the human cytochrome *c* oxidase. While counterintuitive, there already exist several reports of VDAC from various origins (*Saccharomyces cerevisiae*, *Neurospora crassa*, human, mouse) being able to recognize or interact with heterologous proteins. Some hexokinase isoforms bind VDAC across species (*49*−*51*), like do creatine kinase (*47*) and other modulating molecules (*21*, *48*, *52*, *53*). While VDAC sequences from yeast and human are not identical (slightly less than 50% similarity), it can thus be significant that YVDAC is at least as effective as HVDAC1 in activating the COX enzyme. Besides, most of the VDAC protein sequence is used for its transmembrane strands leaving only a few short interacting loops with presumably only a few essential interacting residues.

A possible way to evidence that such interaction do occur in vivo would be to measure COX activity in VDAC transgene animals. It is worth to note that Wu and co-workers (*54*) did report that VDAC1- and VDAC2-deficient mice cells exhibited reduced cytochrome *c* oxidase activity. While not straightforwardly interpretable, such data would be consistent with ours. Our data could provide a hypothetical

mechanism for the cognitive deficits consecutive to decreased COX activity and measured in such transgene mice lacking MVDAC1 or MVDAC2 (*55*).

Whether this VDAC−COX interaction is physiologically relevant has yet to be formally proven, but the facts that we could record it in four different and independent sets of experimental conditions and that this interaction is isoform-specific and consistent with transgene data render it plausible. Given the important roles of both proteins, metabolism, apoptosis, and cell differentiation, the implications of such interaction should be further widely studied and extended.

ACKNOWLEDGMENT

Dr. Verkhovsky (Helsinki, Finland) kindly provided the crystal grade cytochrome *c* oxidase.

REFERENCES

1. Rostovtseva, T., and Colombini, M. (1996) ATP flux is controlled by a voltage-gated channel from the mitochondrial outer membrane, *J. Biol. Chem. 271*, 28006−28008.
2. Colombini, M., Blachly-Dyson, E., and Forte, M. (1996) VDAC, a channel in the outer mitochondrial membrane, *Ion Channels 4*, 169−202.
3. Colombini, M. (2004) VDAC: the channel at the interface between mitochondria and the cytosol, *Mol. Cell. Biochem. 256*−*257*, 107−115.
4. Desagher, S., and Martinou, J. C. (2000) Mitochondria as the central control point of apoptosis, *Trends Cell Biol. 10*, 369−377.
5. Vander Heiden, M. G., Li, X. X., Gottleib, E., Hill, R. B., Thompson, C. B., and Colombini, M. (2001) Bcl-xL promotes the open configuration of the voltage-dependent anion channel and metabolite passage through the outer mitochondrial membrane, *J. Biol. Chem. 276*, 19414−19419.
6. Crompton, M. (1999) The mitochondrial permeability transition pore and its role in the cell death, *Biochem. J. 341*, 233−249.
7. Zamzami, N., and Kroemer, G. (2001) The mitochondrion in apoptosis: how Pandora's box opens, *Nat. Rev. Mol. Cell Biol. 2*, 67−71.
8. Cesura, A. M., Pinard, E., Schubenel, R., Goetschy, V., Friedlein, A., Langen, H., Polcic, P., Forte, M. A., Bernardi, P., and Kemp, J. A. (2003) The voltage-dependent anion channel is the target for a new class of inhibitors of the mitochondrial permeability transition pore, *J. Biol. Chem. 278*, 49812−49818.
9. Linden, M., and Karlsson, G. (1996) Identification of porin as a binding site for MAP2, *Biochem. Biophys. Res. Commun. 218*, 833−836.
10. Kusano, H., Shimizu, S., Koya, R. C., Fujita, H., Kamada, S., Kuzumaki, N., and Tsujimoto, Y. (2000) Human gelsolin prevents apoptosis by inhibiting apoptotic mitochondrial changes via closing VDAC, *Oncogene 19*, 4807−4814.
11. Xu, X., Forbes, J. G., and Colombini, M. (2001) Actin modulates the gating of *Neurospora crassa* VDAC, *J. Membr. Biol. 180*, 73−81.
12. Gonzalez-Gronow, M., Kalfa, T., Johnson, C. E., Gawdi, G., and Pizzo, S. V. (2003) The voltage-dependent anion channel is a receptor for plasminogen kringle 5 on human endothelial cells, *J. Biol. Chem. 278*, 27312−27318.
13. Sun, J., and Liao, J. K. (2002) Functional interaction of endothelial nitric oxide synthase with a voltage-dependent anion channel, *Proc. Natl. Acad. Sci. U.S.A. 99*, 13108−13113.
14. Xu, X., and Colombini, M. (1996) Self-catalyzed insertion of proteins into phospholipid membranes, *J. Biol. Chem. 271*, 23675−23682.
15. Zizi, M., Thomas, L., Blachly-Dyson, E., Forte, M., and Colombini, M. (1995) Oriented channel insertion reveals the motion of a transmembrane beta strand during voltage gating of VDAC, *J. Membr. Biol. 144*, 121−129.
16. De Pinto, V., Prezioso, G., and Palmieri, F. (1987) A simple and rapid method for the purification of the mitochondrial porin from mammalian tissues, *Biochim. Biophys. Acta 905*, 499−502.
17. Palmieri, F., and De Pinto, V. (1989) Purification and properties of the voltage-dependent anion channel of the outer mitochondrial membrane, *J. Bioenerg. Biomembr. 21*, 417−425.
18. Colombini, M. (1979) A candidate for the permeability pathway of the outer mitochondrial membrane, *Nature 279*, 643−645.
19. Blachly-Dyson, E., Peng, S., Colombini, M., and Forte, M. (1990) Selectivity changes in site-directed mutants of the VDAC ion channel: structural implications, *Science 247*, 1233−1236.
20. Wunder, U. R., and Colombini, M. (1991) Patch clamping VDAC in liposomes containing whole mitochondrial membranes, *J. Membr. Biol. 123*, 83−91.
21. Elkeles, A., Breiman, A., and Zizi, M. (1997) Functional differences among wheat voltage-dependent anion channel (VDAC) isoforms expressed in yeast, *J. Biol. Chem. 272*, 6252−6260.
22. Cooper, M. A., Hansson, A., Lofas, S., and Williams, D. H. (2000) A vesicle capture sensor chip for kinetic analysis of interactions with membrane-bound receptors, *Anal. Biochem. 277*, 196−205.
23. Erb, E. M., Chen, X., Allen, S., Roberts, C. J., Tendler, S. J., Davies, M. C., and Forsen, S. (2000) Characterization of the surfaces generated by liposome binding to the modified dextran matrix of a surface plasmon resonance sensor chip, *Anal. Biochem. 280*, 29−35.
24. Lasonder, E., Schellekens, G. A., and Welling, G. W. (1994) A fast and sensitive method for the evaluation of binding of phage clones selected from a surface displayed library, *Nucleic Acids Res. 22*, 545−546.
25. Anderson, S., Bankier, A. T., Barrell, B. G., de Bruijn, M. H., Coulson, A. R., Drouin, J., Eperon, I. C., Nierlich, D. P., Roe, B. A., Sanger, F., Schreier, P. H., Smith, A. J., Staden, R., and Young, I. G. (1981) Sequence and organization of the human mitochondrial genome, *Nature 290*, 457−465.
26. Tsukihara, T., Aoyama, H., Yamashita, E., Tomizaki, T., Yamaguchi, H., Shinzawa-Itoh, K., Nakashima, R., Yaono, R., and Yoshikawa, S. (1996) The whole structure of the 13-subunit oxidized cytochrome *c* oxidase at 2.8 Å, *Science 272*, 1136−1144.
27. Stieglerova, A., Drahota, Z., Ostadal, B., and Houstek, J. (2000) Optimal conditions for determination of cytochrome *c* oxidase activity in the rat heart, *Physiol. Res. 49*, 245−250.
28. Sinjorgo, K. M., Durak, I., Dekker, H. L., Edel, C. M., Bieleman, A. H., Back, N. B., Hakvoort, T. B., and Muijsers, A. O. (1987) The effect of detergents on bovine cytochrome *c* oxidase: a kinetic approach, *Biochim. Biophys. Acta 893*, 241−250.
29. Blachly-Dyson, E., Song, J., Wolfgang, W. J., Colombini, M., and Forte, M. (1997) Multicopy suppressors of phenotypes resulting from the absence of yeast VDAC encode a VDAC-like protein, *Mol. Cell. Biol. 17* (10), 5727−5738.
30. Capaldi, R. A. (1990) Structure and function of cytochrome *c* oxidase, *Annu. Rev. Biochem. 59*, 569−596.
31. Cooper, C. E., Nicholls, P., and Freedman, J. A. (1991) Cytochrome *c* oxidase: structure, function, and membrane topology of the polypeptide subunits, *Biochem. Cell Biol. 69*, 586−607.
32. Wu, W., Schmidt, T. R., Goodman, M., and Grossman, L. I. (2000) Molecular evolution of cytochrome *c* oxidase subunit I in primates: is there coevolution between mitochondrial and nuclear genomes?, *Mol. Phylogenet. Evol. 17*, 294−304.
33. Casadio, R., Jacoboni, I., Messina, A., and De, P. V. (2002) A 3D model of the voltage-dependent anion channel (VDAC), *FEBS Lett. 520*, 1−7.
34. Song, J., Midson, C., Blanchly-Dyson, E., Forte, M., and Colombini, M. (1998) The topology of VDAC as probed by biotin modification, *J. Biol. Chem. 273*, 24406−24413.
35. Yu, C., Yu, L., and King, T. E. (1975) Studies on cytochrome oxidase. Interactions of the cytochrome oxidase protein with phospholipids and cytochrome *c*, *J. Biol. Chem. 250*, 1383−1392.
36. Speck, S. H., Dye, D., and Margoliash, E. (1984) Single catalytic site model for the oxidation of ferrocytochrome *c* by mitochondrial cytochrome *c* oxidase, *Proc. Natl. Acad. Sci. U.S.A. 81*, 347−351.
37. Garber, E. A., and Margoliash, E. (1990) Interaction of cytochrome *c* with cytochrome *c* oxidase: an understanding of the high- to low-affinity transition, *Biochim. Biophys. Acta 1015*, 279−287.
38. Sinjorgo, K. M., Steinebach, O. M., Dekker, H. L., and Muijsers, A. O. (1986) The effects of pH and ionic strength on cytochrome *c* oxidase steady-state kinetics reveal a catalytic and a non-catalytic interaction domain for cytochrome *c*, *Biochim. Biophys. Acta 850*, 108−115.

39. Shikita, M., Fahey, J. W., Golden, T. R., Holtzclaw, W. D., and Talalay, P. (1999) An unusual case of 'uncompetitive activation' by ascorbic acid: purification and kinetic properties of a myrosinase from *Raphanus sativus* seedlings, *Biochem. J. 341* (Pt 3), 725−732.
40. Palmi, M., Youmbi, G. T., Fusi, F., Sgaragli, G. P., Dixon, H. B., Frosini, M., and Tipton, K. F. (1999) Potentiation of mitochondrial Ca^{2+} sequestration by taurine, *Biochem. Pharmacol. 58*, 1123−1131.
41. Phillips, M. F., and Mantle, T. J. (1991) The initial-rate kinetics of mouse glutathione S-transferase YfYf. Evidence for an allosteric site for ethacrynic acid, *Biochem. J. 275* (Pt 3), 703−709.
42. Blachly-Dyson, E., Zambronicz, E. B., Yu, W. H., Adams, V., McCabe, E. R., Adelman, J., Colombini, M., and Forte, M. (1993) Cloning and functional expression in yeast of two human isoforms of the outer mitochondrial membrane channel, the voltage-dependent anion channel, *J. Biol. Chem. 268*, 1835−1841.
43. Cheng, E. H., Sheiko, T. V., Fisher, J. K., Craigen, W. J., and Korsmeyer, S. J. (2003) VDAC2 inhibits BAK activation and mitochondrial apoptosis, *Science 301*, 513−517.
44. Chandra, D., Choy, G., Daniel, P. T., and Tang, D. G. (2005) Bax-dependent regulation of Bak by voltage-dependent anion channel 2, *J. Biol. Chem. 280*, 19051−19061.
45. Adams, V., Griffin, L., Towbin, J., Gelb, B., Worley, K., and McCabe, E. R. (1991) Porin interaction with hexokinase and glycerol kinase: metabolic microcompartmentation at the outer mitochondrial membrane, *Biochem. Med. Metab. Biol. 45*, 271−291.
46. Brdiczka, D., Kaldis, P., and Wallimann, T. (1994) In vitro complex formation between the octamer of mitochondrial creatine kinase and porin, *J. Biol. Chem. 269*, 27640−27644.
47. Schlattner, U., Dolder, M., Wallimann, T., and Tokarska-Schlattner, M. (2001) Mitochondrial creatine kinase and mitochondrial outer membrane porin show a direct interaction that is modulated by calcium, *J. Biol. Chem. 276*, 48027−48030.
48. Xu, X., Decker, W., Sampson, M., Craigen, W., and Colombini, M. (1999) Mouse VDAC isoforms expressed in yeast: channel properties and their roles in mitochondrial outer membrane permeability, *J. Membr. Biol. 170*, 89−102.
49. Azoulay-Zohar, H., and Aflalo, C. (1999) Binding of rat brain hexokinase to recombinant yeast mitochondria: identification of necessary molecular determinants, *J. Bioenerg. Biomembr. 31*, 569−579.
50. Azoulay-Zohar, H., and Aflalo, C. (2000) Binding of rat brain hexokinase to recombinant yeast mitochondria: identification of necessary physico-chemical determinants, *Eur. J. Biochem. 267*, 2973−2980.
51. Nakashima, R. A., Mangan, P. S., Colombini, M., and Pedersen, P. L. (1986) Hexokinase receptor complex in hepatoma mitochondria: evidence from *N*,*N*′-dicyclohexylcarbodiimide-labeling studies for the involvement of the pore-forming protein VDAC, *Biochemistry 25*, 1015−1021.
52. Liu, M. Y., and Colombini, M. (1991) Voltage gating of the mitochondrial outer membrane channel VDAC is regulated by a very conserved protein, *Am. J. Physiol. 260*, C371−C374.
53. Zizi, M., Forte, M., Blachly-Dyson, E., and Colombini, M. (1994) NADH regulates the gating of VDAC, the mitochondrial outer membrane channel, *J. Biol. Chem. 269*, 1614−1616.
54. Wu, S., Sampson, M., Decker, W., and Craigen, W. (1999) Each mammalian mitochondrial outer membrane porin protein is dispensable: effects on cellular respiration, *Biochem. Biophys. Acta 1452*, 68−78.
55. Scaglia, N., Cai, Z., Anflous, K., Armstrong, D., Levin, M., Sweatt, J. D., and Craigen, W. (2002) Mitochondrial porin deficient mice: a murine model of Mendelian respiratory chain defects and encephalopathy, Workshop, Systems Biology Approaches to Health Care: Mitochondrial Proteomics, presented Sept 17, 2002.

BI050674S